Methods

A published adult human PBPK model for BDCM (Kenyon *et al.*, 2016a) was re-parameterized for three pediatric age groups: 0-30 days (neonate), 31-90 days (infant) and 91days -2 years of age (toddler). These intervals were selected based on the age groups identified in Johnsrud *et al.* (2003) that correspond to the CYP2E1 developmental trajectory that minimizes differences within while maximizing differences between age groups. The pediatric CYP2E1 hepatic protein expression data are described in greater detail in the supplemental material and are part of a larger published database for XME ontogeny (McCarver et al., 2017).

The model structure (see Fig. S1) and assumptions have been described in detail elsewhere; this model adequately predicted BDCM blood concentrations in studies of adult volunteers during water use exposures involving drinking, bathing and showering (Kenyon *et al.*, 2016a). Model structure, assumptions and chemical-specific parameters for this analysis are the same as those used previously (Kenyon *et al.,* 2016 a, b). Adult physiological parameters are provided in Table 1, and many are the same as those used previously with some specific exceptions. Alveolar ventilation rate (QPC), alveolar deadspace, ratio of QPC to cardiac output and fat volume were updated to use the more comprehensive sources used for pediatric parameters (Brochu *et al*., 2006, 2011, 2012, Brown *et al*., 1997, Haddad *et al.*, 2001). Organ volumes (Table 1) for pediatric age groups were calculated on the basis of the equations presented in Haddad *et al.* (2001) with total body fat calculated on the basis of Price *et al.* (2003). Blood flows for pediatric populations were primarily derived from Edginton *et al.* (2006) and other physiological parameters were obtained from the literature as detailed in footnotes to Table 1 (Brochu *et al.*, 2006, 2011, 2012; Laurent *et al.*, 2007, Saito *et al.*, 2015).

Chemical-specific parameters are provided in Table 2. Partition coefficients were treated as invariant across age groups. Available data indicate that blood:air partition coefficients for volatile organic compounds do not differ between adult and pediatric populations (Mahale *et al.*, 2007). In addition, tissue lipid and water composition does not differ substantively as a function of age from newborn to young adult for healthy tissues (White *et al*., 1991). Other chemical-specific parameters were the same as used in our previous analysis (Kenyon *et al.*, 2016b) and treated as invariant across age groups. The Vmax for hepatic CYP2E1-mediated BDCM metabolism (VmaxBDCM) in units of µg/h-kg was made specific for each age group and calculated within the model code during each simulation using the equation:

VmaxBDCM = *in vitro* Vmax x MPPGL x CYP2E1 x FVL (1)

where the *in vitro* Vmax is in units of µg/h-pmol CYP2E1 (Table 2), MPPGL is in units of mg MSP/g liver, CYP2E1 is in units of pmol CYP2E1 protein/mg MSP and FVL is in units of g liver/kg BW (Table 3). Distributional characteristics are provided in Table 3 and were based on data from Johnsrud *et al.* (2003), McCarver *et al.* (2017), Lipscomb *et al.* (1997, 2003a, b) and Young *et al.* (2009). These data sets were selected because the complete original data were available enabling calculation of all needed distributional descriptors (Table 3) and descriptive statistics (Table S1). Because subject age was available in these data sets, but measured data for MPPGL were not collected, MPPGL was estimated for each subject using the age-based equation published by Barter *et al.* (2008). FVL, MPPGL and CYP2E1 were assumed to vary independently (Lipscomb *et al.,* 2003a, b).

Distributions for FVL and MPPGL, normal and lognormal, respectively, were selected consistent with U.S. EPA (2011b). Lower and upper bounds for FVL and MPPGL were set at the minimum and maximum values from the original data sets. Distributions for CYP2E1 were

fitted using the SAS SEVERITY procedure (SAS 2013) because 8 of the 42 neonatal CYP2E1 protein expression measurements were below the limit of detection. The SAS SEVERITY procedure is appropriate when there are below-detection, left-censored data and uses maximum likelihood to estimate distribution parameters. Lognormal and gamma distributions were considered for each of the age groups using the Akaike information criterion (AIC), corrected AIC (AICC), and Bayesian information criterion (BIC) as the selection criteria. For consistency, the gamma distribution was selected for all age groups because it was either a better fit (neonates) or virtually indistinguishable from the lognormal distribution (Table S2). Input parameter distributions and values are given in Table 3.

Monte Carlo analysis was used to assess effects of variability in model input parameters, CYP2E1, MPPGL and FVL, on PK outcomes (Figure 1). The Monte Carlo method was used to randomly sample CYP2E1, MPPGL and FVL from defined distributions (Table 3) to estimate Vmax for BDCM within the model. Running the model for 10,000 iterations provided PK outcome data for which summary descriptive statistics were calculated. Two exposure scenarios (single 0.05-liter drink or 20-minute bath) were simulated to encompass the range of relevant exposure routes for BDCM (Kenyon *et al.*, 2016b) at typical (5 μg/L) and plausibly high (20 μg/L) water concentrations across age groups; total simulation length was 2 hours for all scenarios. PK model outcomes evaluated were area under the curve (AUC) for BDCM in venous blood (AUCv), amount of BDCM metabolized in liver (AML), maximum BDCM concentration in blood (CVmax) and maximum concentration of BDCM in exhaled breath (CalvMax). Model responses selected for evaluation were those that were either likely to be measured in water use studies (blood concentration, exhaled breath) as well as pharmacokinetically-relevant measures

of internal dose (AUCv, AML). The workflows for the methods used in this analysis are illustrated in Figure 1.

Global sensitivity analysis (GSA) was performed in AcslXtreme 3.0.2.1 using the Morris method (Morris, 1991) to provide a relative ranking of importance for all model parameters. To implement the Morris GSA method in AcslXtreme, it is necessary to set ranges for input parameters that are allowed to vary under the assumption of a uniform distribution, which is considered appropriate for a screening level analysis. For physiological parameters, partition coefficients and the dermal absorption coefficient, ranges were set as ± one standard deviation from the average value used in the model (Tables 1 and 2) assuming a coefficient of variation of 30%. This assumption has been used in reverse dosimetry applications of PBPK models (e.g., Tan *et al.* 2007). Variation in VmaxBDCM was set based on available data (Table 3) and the range of variation for all other chemical-specific parameters was as described in Kenyon *et al.* (2016b). Algorithmic settings used in the analysis were 100, 25 and 1000, for p, jump, and Ns, respectively. P is the number of values in discretized parameter range (divides parameter range into p-1 ranges or hypercubes); jump is the step size in computing effects (effectively computing a number of local sensitivities); Ns is the number of samples (AEgisTechnologies 2010). These algorithmic settings were selected to optimize analysis performance; i.e., multiple test runs were done until no changes were seen in the overall ranking.

Results

Pharmacokinetic outcome results from the Monte Carlo simulations for oral exposure at 5 µg/L across age groups are shown in Figures 2A and B and Table 4 for AUCv, AML, and CVmax, respectively. Corresponding figures and tables for the 20 µg/L oral exposure are in

supplemental material (Figures S2A and S2B, Table S3). For all PK outcomes, variability was greater in the neonate compared to other pediatric age groups or adults as assessed by coefficient of variation (%CV) and ratio of 95th to 5th percentile. For AUCv, CVmax and CalvMax, concentrations were higher in pediatric age groups compared to adults due to the smaller body mass in the former (e.g. 3.81 kg neonate vs. 80.8 kg adult, Table 1), i.e., the same absolute amount is distributed into a smaller volume. For CalvMax, the % CV and ratio of 95th to 5th percentile values are the same as CVmax, and the concentrations are uniformly ~17-fold lower across age groups for CalvMax (model results not shown) compared to CVmax. The total amount of BDCM metabolized in liver (Fig 2B) was similar across age groups because metabolism is not saturated under this oral exposure scenario and overall liver metabolic capacity is not exceeded (Kenyon *et al.*, 2016a). Results were essentially the same for the 20 µg/L exposure scenarios; the observed dose-dependent differences in the parameters were ~ 4-fold because the processes of absorption, disposition, metabolism and excretion are within the linear range at this exposure level.

Results from the Monte Carlo simulations for bathing exposure at 5 µg/L across age groups are shown in Figures 3A and B and Table 5 for AUCv, AML, and CVmax, respectively. Corresponding figures and tables for the 20 µg/L bathing exposure are in supplemental material (Figures S3A and S3B, Table S4). As with the oral exposure, all PK outcomes for bathing exposure displayed greater variability in the neonate compared to other pediatric age groups and adults based on %CV and ratio of 95th to 5th percentile values. However, compared to oral exposure, the extent of variability was not as large between PK outcomes. Concentrations for AUCv, and CVmax were generally greater for younger age groups although cross-age group differences were not substantial. For CalvMax, the % CV and ratio of 95th to 5th percentile

values are the same as CVmax, and the concentrations are uniformly ~17-fold lower across age groups for CalvMax (model results not shown) compared to CVmax. The total amount of BDCM metabolized in liver was greater in adults compared to pediatric age groups (Fig. 3B) due to relatively greater uptake of parent chemical and delivery to the liver via combined dermal and inhalation exposure for adults during bathing.

Quantitative results for GSA using the Morris screening method are illustrated graphically in Figures 4 (AUCv) and 5 (AML) for oral and Figures 6 (AUCv) and 7(AML) for bathing exposure to 5 μg/L BDCM in water; the A and B panels in these figures reflect neonates and adults, respectively, because these two age groups show the largest and smallest variation in PK outcomes, respectively. In these figures, the mean sensitivity coefficient for each parameter (averaged over the time period of the simulation) is plotted on the x-axis (μ) and the corresponding standard deviation (σ) is plotted on the y-axis to display the overall screening level GSA results. This presentation format provides an overall quantitative sense of how parameters compare to each other in terms of their relative influence on the PK outcome of interest (McNally *et al.* 2011). Further detail is presented in corresponding tables (S5-S8) in the supplemental material. For oral exposure in both neonates and adults, the parameters that were most influential for AUCv were those governing absorption (KABDCM), relative liver mass (FVL) and biotransformation via the CYP2E1 pathway (CYP2E1, KM1BDCM). These same parameters also were influential for the amount of BDCM metabolized in liver (AML). CYP2E1 was the most influential parameter for AUCv and AML for both adults and neonates, although by comparison this was more strongly evident in neonates for AML. For the bathing exposure scenario, a number of parameters were highly influential for both AUCv and AML in neonates and adults; the parameters identified as influential in adults were similar to previous sensitivity

analysis for this model (Kenyon *et al.*, 2016a). What is evident for both neonatal AUCv and AML PK outcomes compared to adults is the relatively higher ranking of CYP2E1 in neonates. MPPGL was generally in the middle third of relative rankings among parameters for all PK outcomes in both adults and neonates.

Discussion

Our results clearly demonstrate that variability in the development of hepatic XMEs in early childhood contributes to greater variability in predicted pharmacokinetic outcomes for early life stages compared to adults. The PBPK modeling framework is a particularly strong approach for this purpose because it incorporates relevant environmental exposures and known pediatric-specific physiological and molecular parameters using a validated model that estimates both internal dose measures and biomarkers of exposure. Use of this framework allowed for the integration of diverse information to provide a physiologically and environmentally realistic context in which to evaluate the impact of observed interindividual differences in XME ontogeny. This framework also can account for other physiological factors that may differ across life stages (Yoon and Clewell, 2016) including plasma binding protein expression (e.g., Sethi *et al.*, 2016) and hepatic drug transporters (Prasad *et al.*, 2016, Thomson et al., 2016).

In this case study, PK outcomes exhibited greater variability (as assessed by %CV and ratio of 95^{th} to 5^{th} percentile values) at younger postnatal ages for both oral and bathing exposure, although variability was generally less pronounced for the bathing exposure scenario. For the oral exposure scenario, variation in hepatic scaling factors for pediatric age groups had the greatest impact on pharmacokinetic outcomes (AUCv, CVmax, CalvMax) compared to adults. There was also greater variability in neonates compared to adults for hepatic biotransformation (AML), although it was relatively less compared to other pharmacokinetic outcomes. The

overall findings in adults were similar to our earlier work in adults (Kenyon *et al.*, 2016b). The most likely explanation for the relatively lower variation across age groups in AML compared to other PK outcomes is that at typically low environmental exposure concentrations, hepatic biotransformation is not saturated (Kenyon *et al.*, 2016a); delivery of parent chemical to liver in blood is the rate limiting step in hepatic biotransformation under these exposure conditions. For bathing exposures, there was relatively greater variability in neonates compared to adults, although the magnitude of variation (% CV, ratio of 95^{th} to 5^{th} percentiles) was relatively less compared to oral exposures. Lesser impact for bathing compared to oral exposures is partially attributable to the physiology of inhalation and dermal absorption; compounds absorbed into the systemic circulation are not immediately subject to first-pass metabolism in liver or intestine, as are compounds delivered orally (Lehman-McKeeman, 2013).

Global sensitivity analysis for all model parameters using a screening method such as Morris (1991) provides a relative sense of specific parameter influence for a given exposure scenario and PK outcome for individual age groups; another advantage of GSA in general is that it allows incorporation of observed parameter variability (McNally *et al.*, 2011). In this analysis we looked at neonatal and adult groups because these groups demonstrated the largest and smallest predicted variability in PK outcomes, respectively, based on the Monte Carlo analysis. For neonates, CYP2E1 specific content was consistently either the most influential parameter or in the top 10% of influential parameters for all PK outcomes for both oral and bathing exposure scenarios. In adults, this was also true for oral, but not bathing exposure. Relative liver mass (FVL) was generally in the top 1/3 of influential parameters for neonates in all cases, but for adults, only for oral, not bathing exposure.

A novel aspect of our model is use of the gamma distribution without lower and upper bounds to parameterize CYP2E1. Most PBPK models assume a lognormal distribution for XME content or biochemical parameters such as Vmax (e.g. Lipscomb et al, 2003a, b; U.S. EPA, 2011b; Tan et al., 2007). Use of the gamma distribution in our analysis for CYP2E1 parameterization has both statistical, and biological rationale. Based on AIC, AICC, and BIC information criteria, gamma distributions gave better fits for the neonate and infant CYP2E1 data than lognormal distributions and the lognormal distribution was not compellingly superior to the gamma distribution for other age groups (Table S2). The gamma CYP2E1 parameterization without truncation for neonates has an important biological basis in that it supports representation of no functional protein present, the mode for neonate CYP2E1 in the Johnsrud *et al*. (2003) data. An empirical assessment of the effect of the seed used to randomly sample CYP2E1 for model input to the Monte Carlo analysis for neonate oral exposure demonstrated that the ratio of 95th to 5th percentiles was relatively stable in contrast to the ratio of the max to the min (Table S9).

In general, MPPGL ranked in the middle third or lower among influential parameters for both neonates and adults. The relatively lesser influence of MPPGL in our model, in part, corresponds to the dependence of its input distribution on values predicted by the 2008 Barter regression equation, which is a function of age. One limitation of the Barter equation is that it accounted for only 10% of the variability in observed data used in its development (Barter *et al.*, 2008). Using this equation results in less variability in MPPGL in younger age groups which also contributes to making this parameter relatively lower in influence on PK outcomes in general, particularly in neonates. Reassuringly, recently published measurements of MPPGL in

neonates as determined using the total cytochrome P450 method (De Bock *et al.*, 2014) fall within the range of values predicted by the equation of Barter *et al.* (2008).

Another source of uncertainty in model outputs is the assumption that FVL, MPPGL and CYP2E1 are independent. If this assumption is inaccurate, the model outputs may reflect excess variability (Thomas *et al.*, 1996). Chemical-specific model parameters were treated as invariant across age groups and there is data to support this assumption for partition coefficients (Mahale *et al.*, 2007; White *et al.*, 1991). However, in the case of the skin diffusion coefficient (KABDCM), evidence suggests that the skin of the neonate is more fragile and permeable to pharmaceuticals compared to adult skin (Blume-Peytavi *et al.*, 2016). This could result in increased absorption of BDCM into the systemic circulation following dermal exposure in pediatric populations.

This work was possible because of the existence of a large data base on pediatric XME expression in liver spanning both pre-natal and early childhood life stages for a large array of enzymes (McCarver *et al.*, 2017). The unique value of such a database is that the information can be utilized to predict biotransformation and its associated variability for pediatric age groups for any chemical provided the XMEs responsible for its biotransformation and an *in vitro* rate of biotransformation for the specific chemical are known. Further classifying XMEs according to expression trajectories during pre- and post-natal development can facilitate identification of chemicals that are a higher priority for evaluation when considered together with information on exposure potential in pediatric populations.

Another PBPK-based risk analysis application for XME ontogeny data was demonstrated by Nong *et al.* (2006). These authors assessed the impact of variability in both physiological parameters and CYP2E1 expression on AUC for toluene in blood using a scenario of 1 ppm

toluene exposure for 24 hours. Using the 5th, 50th, and 95th percentiles for predicted AUC, Nong *et al.* (2006) calculated intragroup and adult-child factors; the intragroup variability factor was calculated as the ratio of the 95th percentile value over the 50th percentile value for the same age group, and the adult-child variability factor was calculated as the ratio of the 95th percentile value for the child over the 50th percentile value for the adult. Intragroup factors varied between 1.07 and 1.48 and adult-child variability factors ranged from 3.88 to 1.35 from neonate to adolescent. The intragroup variability factor provides an another way to compare variability between age groups, much as the %CV and ratio of 95th to 5th percentile used in Tables 4 and 5, and Figures 2,3, S2, S3 in the present study. The calculated adult-child variability factor is specific for this chemical exposure scenario (inhalation) and dose metric (AUC). The adult-child variability factor is analogous to the PK portion of the default uncertainty factor for interindividual variability (UF_HTK=3) and has also been used in risk analysis as a chemical-specific adjustment factor (CASF; IPCS, 2005) or data-derived extrapolation factor (DDEF; USEPA, 2014) to avoid the application of default uncertainty factors.

We performed a similar analysis to that of Nong *et al.* (2006) for AUCv (Table 6) and AML (Table 7) based on both oral and bathing exposures for BDCM (1) to compare general intragroup trends across lifestages and (2) to examine the impact of exposure scenario and choice of internal dose metric on the adult-child variability factor. For AUCv (Table 6), we observed increased intragroup variability at younger ages following the same trend as Nong et al. (2006) for both bathing and oral exposures with the differences between scenarios being more pronounced for oral exposure (see also Figures 2A and 3A). For AML all intragroup variability factors approach unity. As discussed in the context of data in Figures 2B and 3B, this is due to metabolism being blood flow limited at environmental exposure levels.

The adult-child variability factor differed substantially between dose metrics and exposure scenarios. Results in Table 6 for parent BDCM exposures (AUCv) differ appreciably between exposure routes. These values demonstrate adult-child factor values for the bathing scenario that range from near-unity (toddler) to a value roughly similar to the assumed default value for toxicokinetic differences among humans (neonate), while values for the oral route may exceed five hundred-fold. Differences for the oral route likely reflect the overall higher VmaxC (Table S1) and overall metabolic capacity of the adult compared to that of the neonate, combined with a higher internal dose developed following the more temporally-concentrated oral exposure scenario as compared with the bathing scenario. Overall trends across age groups were similar to those reported by Nong *et al.* (2006). Amount metabolized in liver (Table 7) presents a dramatically different picture compared to AUCv. The adult-child factor values for bathing are substantially lower than 1, while adult-child factors for the oral exposure approximate unity. Together, these data suggest minimal differences between adults and younger age groups for this dose metric.

The magnitude of differences observed for the adult-child variability factor across exposure scenarios and dose metrics illustrates the importance of identifying the dose metric of greatest concern and considering multiple routes of exposure when appropriate. In the case of a possible role for BDCM in DBP-associated human bladder cancer, available data suggests that extrahepatic metabolism (i.e., metabolic activation within urothelial cells) is a key carcinogenic event (Ross and Pegram, 2003 and 2004; Cantor et al., 2010). Previous work demonstrated that combined dermal and inhalation exposure results in greater levels of BDCM reaching the systemic circulation compared to ingestion, and thus being available for extrahepatic metabolism (Kenyon *et al.*, 2016a; Leavens et al., 2007, Backer et al., 2000). Taken together, these data

highlight the importance of evaluating lifetime, age-specific exposure across multiple routes of exposure to provide the most complete analysis of BDCM internal exposure and hence risk.

When data on the developmental trajectory is available for a variety of XMEs it is also possible to evaluate the impact of transitions in the specific enzymes involved in biotransformation for particular chemicals. For example, Yang *et al.* (2006) modeled predicted changes in methadone kinetics in pediatric populations 0-24 months of age compared to adults based on measured variability and changes in CYP3A4, CYP3A5 and CYP3A7 expression levels, as well as other physiological parameters using a PBPK model. In addition to the CYP3A family of enzymes (Stevens *et al.*, 2003), similar transitions have been reported for FMO1 transitioning to FMO3 (Koukourtiaki *et al.*, 2002). In the case of BDCM, CYP2E1 is the predominant biotransformation enzyme at low substrate concentrations, but both CYP1A2 and CYP3A4 can make substantial contribution to biotransformation at higher substrate concentrations. This raises the question of whether these other enzymes could augment BDCM metabolism if CYP2E1 is not expressed or expressed only at very low levels. Both CYP3A4 and CYP1A2 were measured in the same pediatric livers from which CYP2E1 data used in this study were obtained (McCarver *et al.*, 2017). However, both CYP3A4 and CYP1A2 protein levels were low in the neonate and increased only slowly during the first 6 months to 15 months of life, respectively (Stevens *et al.*, 2003; Song *et al.*, 2017). Thus, in the absence of sufficient CYP2E1 enzyme, substantial CYP3A4 or CYP1A2 contributions to BDCM metabolism would only be predicted in the older age groups and adults.

Our results also demonstrate the potential for higher internal extrahepatic exposure to BDCM in neonates and infants compared to adults (as shown by predicted CvMax and AUCv values), which could be toxicologically significant depending upon the chemical. BDCM is

carcinogenic in rodents with oral gavage exposure resulting in kidney carcinomas in both rats and mice, as well as large intestine carcinomas in rats (USEPA 2005). An increased risk for bladder and colon cancer have been reported in epidemiologic studies (Villanueva et al. 2014), with the most compelling evidence being for bladder cancer (Cantor et al. 2010). For environmental contaminants such as BDCM concerns related to metabolism in both target and non-target tissues can be critical (Ross and Pegram, 2004), and overall there is a paucity of data needed to scale *in vitro* metabolism data to the *in vivo* situation for extrahepatic metabolism, and to characterize the associated variability.

In summary, this work demonstrates that variation observed in XME expression in early life results in greater predicted variability in PK outcomes compared to adults across multiple PK outcomes and routes of exposure. That this variability is observed during simulation of environmentally relevant exposures makes a strong case for its explicit quantitative consideration when performing child-specific risk analyses.

DISCLAIMER

The research described in this manuscript has been reviewed by the National Health and Environmental Effects Research Laboratory, U. S. Environmental Protection Agency and approved for publication. Approval does not signify that the contents necessarily reflect the views and policies of the agency nor does the mention of trade names or commercial products constitute endorsement or recommendation for use.

ACKNOWLEDGEMENTS

Parts of this work at an earlier stage of development were presented at the 2017 Society of Toxicology Meeting. We thank our colleagues at U.S. EPA/ORD/NCEA and NCCT for their thorough review and helpful suggestions.

REFERENCES

AEgis Technologies. (2010). AcslX Optimum User's Guide. AEgis Technologies: Huntsville, AL.

Backer L.C., Ashley D.L., Bonin M.A., Cardinali F.L., Kieszak S.M., and Wooten J.V. (2000). Household exposures to drinking water disinfection by-products: whole blood trihalomethane levels. J. Exp. Anal. Environ. Epidemiol. **10**, 321-326.

Barter Z.E., Chowdry J.E, Harlow J.R., Snawder J.E., Lipscomb J.C., and Rostami-Hodjegan A. (2008). Covariation of human microsomal protein per gram of liver with age: absence of influence of operator and sample storage may justify inter laboratory data pooling. Drug Metab. Dispos. **36**, 2405–2409.

Batterman S., Zhang L., Wang S., and Franzblau A. (2002). Partition coefficients for the trihalomethanes among blood, urine, water, milk and air. Sci Total Environment **284**, 237-247.

Blume-Peytavi U., Tan J., Tennstedt D., Boralevi F., Fabbrocini G., Torrelo A., Soares-Oliveira R., Haftek M., Rossi A.B., Thouvenin M.D., *et al*. (2016). Fragility of epidermis in newborns, children and adolescents. J. Eur. Acad. Dermatol. Venereol. **30**(Suppl. 4), 3-56.

Brochu P., Ducré-Robitaille J.F., and Brodeur J. (2006). Physiological daily inhalation rates for free-living individuals aged 1 month to 96 years, using data from doubly labeled water measurements: a proposal for air quality criteria, standard calculations and health risk assessment. Human Ecol. Risk Assess. **12**, 675-701.

Brochu P., Brodeur J., and Krishnan K. (2011). Derivation of physiological inhalation rates in children, adults and elderly based on nighttime and daytime respiratory parameters. Inhal. Toxicol. **23**, 74-94.

Brochu P., Brodeur J., and Krishnan K. (2012). Derivation of cardiac output and alveolar ventilation rate based on energy expenditure measurements in healthy males and females. J. Appl. Toxicol. **32**, 564-580.

Brown R.P., Delp M.D., Lindstedt S.L., Rhomberg L.R., and Beliles R.P. (1997). Physiological parameter values for physiologically based pharmacokinetic models. Toxicol. Ind Health **13**, 407-484.

Cantor K.P., Villanueva C.M., Silverman D.T., Figueroa J.D., Real F.X., Garcia-Closas M., Malats N., Chanock S., Yeager M., Tardon A., *et al*. (2010). Polymorphisms in GSTT1, GSTZ1, and CYP2E1, disinfection by-products, and risk of bladder cancer in Spain. Environ. Health Perspect. **118**, 1545-1550.

De Bock L., Boussery K., De Bruyne R., Van Winckel M., Stephenne X., Sokal E., and Van Bocxlaer J. (2014). Microsomal protein per gram of liver (MPPGL) in paediatric biliary atresia patients. Biopharm. Drug Dispos. **35**, 308-312.

Edginton, A.N., Schmitt, W., and Willmann, S. (2006). Development and evaluation of a generic physiologically based pharmacokinetic model for children. Clin. Pharmacokin **45**, 1013-34.

Gehan, E.A. and George, S.L. (1970). Estimation of human body surface area from height and weight. Cancer Chemotherapy Reports Pt 1 54, 225-235.

Haddad, S., Restieri, C., and Krishnan, K. (2001). Characterization of age-related changes in body weight and organ weights from birth to adolescence in humans. J. Toxicol. Environ. Health Pt A **64**, 453-464.

Haddad, S., Tardif, G.C., and Tardif, R. (2006). Development of physiologically based toxicokinetic models for improving the human indoor exposure assessment to water contaminants: trichloroethylene and trihalomethanes. J. Toxicol. Environ. Health Pt. A **69**, 2095-2136.

Hines, R.N. (2008). The ontogeny of drug metabolism enzymes and implications for adverse drug events. Pharmacol. Ther. **118**, 250-267.

Hines, R.N. (2012). Age-dependent expression of human drug-metabolizing enzymes. In AV Lyubimov (ed.), Encyclopedia of Drug Metabolism and Interactions, Chpt. 15, John Wiley & Sons, New York.

International Commission on Radiological Protection (ICRP). (2002). Basic anatomical and physiological data for use in radiological protection: reference values. ICRP 89, ed., J. Valentin, Pergamon Press, Oxford, United Kingdom.

International Programme on Chemical Safety (IPCS). (2005). Chemical-specific adjustment factors for interspecies differences and human variability: guidance document for use of data in dose/concentration-response assessment. World Health Organization, Geneva.

Johnsrud, E.K., Koukouritaki, S.B., Divakaran, K., Brunengraber, L.L., Hines, R.N., and McCarver, D.G. (2003). Human hepatic CYP2E1 expression during development. J Pharmacol. Exp. Ther. (JPET) **307**, 402-407.

Kedderis, G.L. (1997). Extrapolation of in vitro enzyme induction data to humans in vivo. Chem Biol Interact. **107**, 109-21

Kenyon, E.M., Eklund, C., Leavens, T.L., and Pegram, R.A. (2016a). Development and application of a human PBPK model for bromodichloromethane (BDCM) to investigate impacts of multi-route exposure. Journal of Applied Toxicology **36**, 1095-1111.

Kenyon, E.M., Eklund, C., Lipscomb, J.C., and Pegram, R.A. (2016b). The impact of variation in scaling factors on the estimation of internal dose metrics: a case study using bromodichloromethane (BDCM). Toxicol. Mech. Methods **26**, 620-626.

Koukouritaki, S.B., Simpson, P., Yeung, C.K., Rettie, A.E., and Hines, R.N. (2002). Human hepatic flavin-containing monooxygenase 1 (FMO1) and 3 (FMO3) developmental expression. Pediatr. Res. **51**, 236-243.

Laurent, A., Mistretta, F., Bottigioli, D., Dahel, K., Goujon, C., Nicolas, J.F., Hennino, A., and Laurent P.E. (2007). Echographic measurement of skin thickness in adults by high frequency ultrasound to assess the appropriate microneedle length for intradermal delivery of vaccines. *Vaccine* **25**, 6423-6430.

Leavens, T.L., Blount, B.C., DeMarini, D.M., Madden, M.C., Valentine, J.L., Case, M.W., Silva, L.K., Warren, S.H., Hanley, N.M., and Pegram R.A. (2007). Disposition of bromodichloromethane in humans following oral and dermal exposure. *Toxicol. Sci.* **99**, 432-445.

Lehman-McKeeman, L.D. (2013). Absorption, distribution and excretion of toxicants, p.153-184. In: Casarett and Doull's Toxicology, 8th ed. C.D. Klaassen, McGra-Hill, New York.

Lilly, P.D., Andersen, M.E., Ross, T.M., and Pegram, R.A. (1997). Physiologically-based estimation of in vivo rates of bromodichloromethane metabolism. Toxicology **124**, 141-152.

Lipscomb, J.C., Garrett, C.M., andSnawder, J.E. (1997). Cytochrome P450-dependent metabolism of trichloroethylene: interindividual differences in humans. Toxicol. Appl. Pharmacol. **142**, 311-318.

Lipscomb, J.C., Teuschler, L.K., Swartout, J., Popken, D., Cox, T., and Kedderis, G.L. (2003a). The impact of cytochrome P450 2E1-dependent metabolic variance on a risk-relevant pharmacokinetic outcome in humans. Risk Anal. **23**, 1221-38.

Lipscomb, J.C., Teuschler, L.K., Swartout, J., Striley, C.A.F., and Snawder, J.E. (2003b). Variance of microsomal protein and cytochrome P450 2E1 and 3A forms in adult human liver. Toxicology Mechanisms and Methods, **13**, 1, 45-51.

Lipscomb, J.C., and Poet, T.S. (2008). *In vitro* measurements of metabolism for application in pharmacokinetic modeling. Pharmacol. Ther. **118**, 82-103.

Lynberg, M., Nuckols, J.R., Langlois, P., Ashley, D., Singer, P., Mendola, P., Wilkes, C., Krapfl, H., Miles, E., Speight, V., *et al*. (2001). Assessing exposure to disinfection by-products in women of reproductive age living in Corpus Christi, Texas, and Cobb County, Georgia: Descriptive results and methods. Environ. Health Perspect. **109**, 597-604.

McCarver, D.G., Simpson, P.M., Kocarek, T.A., James, M.O., Runge-Morris, M., Stevens, J.C., Yoon, M., and Hines, R.N. (2017). Data from: Developmental expression of drug metabolizing enzymes: Impact on disposition in neonates and young children, DOI: http://dx.doi.org/10.5061/dryad.71pp6

McNally, K., Cotton, R., and Loizou, G.D. (2011). A workflow for global sensitivity analysis of PBPK models. Frontiers Pharmacol. **2**, 1-22.

Morris, M.D. (1991). Factorial sampling plans for preliminary computational experiments. Technometrics **33**, 161-174.

Nong, A., McCarver, D.G., Hines, R.N., and Krishnan, K. (2006). Modeling interchild differences in pharmacokinetics on the basis of subject-specific data on physiology and hepatic CYP2E1 levels: a case study with toluene. Toxicol. Appl. Pharmacol. **214**, 78-87.

Nuckols, J.R., Ashley, D.L., Lyu, C., Gordon, S.M., Hinckley, A.F., and Singer P. (2005). Influence of tap water quality and household water use activities on indoor air and internal dose levels of trihalomethanes. Environ. Health Perspect. **113**, 863-870.

Mahale, D.A., Gearhart, J.M., Grigsby, C.C., Mattie, D.R., Barton, H.A., Lipscomb, J.C., and Cook, R.S. (2007). Age-dependent partition coefficients for a mixture of volatile organic solvents in Sprague-Dawley rats and humans. J. Toxicol. Environ. Health, Pt. A **70**, 1745-1751.

Ploin, D., Schwarzenbach, F., Dubray, C., Nicolas, J.F., Goujon, C., Trong, M.D., and Laurent, P.E. (2011). Echographic measurement of skin thickness in sites suitable for intradermal vaccine injection in infants and children. Vaccine **29**, 8438–42.

Prasad, B., Gaekigk, A., Vrana, M., Gaedigk, R., Leeder, J.S., Salphati, L., Chu, X., Xiao, G., Hop, C.E.C.A., Evers, R., Gan, L., and Juadkat, J.D. (2016). Ontogeny of hepatic drug transporters as quantified by LC-Ms/MS proteomics. Clin. Pharmacol. Ther. **100**, 362-370.

Price, K., Haddad, S., and Krishnan, K. (2003). Physiological modeling of age-specific changes in the pharmacokinetics of organic chemicals in children. J. Toxicol Environ. Health, Pt. A **66**, 417-433.

Ross, M.K., and Pegram, R.A. (2003). Glutathione transferase theta 1-1-dependent metabolism of the water disinfection byproduct bromodichloromethane. *Chem. Res. Toxicol.***16**, 216-226

Ross, M.K., and Pegram, R.A. (2004). In vitro biotransformation and genotoxicity of the drinking water disinfection byproduct bromodichloromethane, DNA binding mediated by glutathione transferase theta 1-1. Toxicol. Appl. Pharmacol. **195**, 166-181.

Saitoh, A., Aizawa, Y., Sato, I., Hirano, H., Sakai, T., and Mori, M. (2015). Skin thickness in young infants and adolescents: applications for intradermal vaccination. Vaccine **33**, 3384-3391.

SAS Institute Inc. (2013). SAS/ETS® 13.1 User's Guide. Cary, NC: SAS Institute Inc.

Sethi, P.K., White, C.A., Cummings, B.S., Hines, R.N., Muralidhara, S., and Bruckner, J.V. (2016). Ontogeny of plasma proteins, albumin and binding of diazepam, cyclosporine, and deltamethrin. Pediatr. Res. **79**, 409-415,

Song, G., Sun, X., Hines, R.N., McCarver, D.G., Lake, B.J., Osimtz, T.G., Creek, M.R., Clewell, H.J., and Young, M. (2017). Determination of human hepatic CYP2C8 and CYP1A2 age-dependent expression to support human health risk assessment for early ages. Drug Metab. Dispos. **45**, 468-475.

Stevens, J.C., Hines, R.N., Gu, C., Koukouritaki, S.B., Manro, J.R., Tandler, P.J., and Zaya, M.J. (2003). Developmental expression of the major human hepatic CYP3A enzymes. J Pharmacol. Exptl. Ther. **307**, 573-582.

Tan, Y.M., Liao K.H., and Clewell, H.J. (2007). Reverse dosimetry: Interpreting trihalomethanes biomonitoring data using physiologically based pharmacokinetic modeling. J. Exp. Sci. Environ. Epidemiol. **17**, 591-603.

Thomas, R.S., Lytle, W.E., Keefe, T.J., Constan, A.A., and Yang, R.S. (1996). Incorporating Monte Carlo simulation into physiologically based pharmacokinetic models using advance continuous simulation language (ACSL): a computational method. Fund. Appl. Toxicol. **31**, 19-28.

Thomson, M.M.S., Hines, R.N., Schuetz, E.G., and Meibohm, B. (2016). Expression patterns of OATP1B1 and OATP1B3 protein in human pediatric liver. Drug Metab. Disp. **44**, 999-1004.

USEPA. (1997). Guiding principles for Monte Carlo analysis. Washington, D.C. Risk Assessment Forum.

USEPA. (2005). Drinking water criteria document for brominated trihalomethanes. EPA-822-R-05-011. Office of Water, Washington D.C.

USEPA. (2008). Child-Specific Exposure Factors Handbook. Office of Research and Development, National Center for Environmental Assessment, Washington, DC. EPA/600/R-06/096F

USEPA. (2011a). Exposure Factors Handbook. Office of Research and Development, National Center for Environmental Assessment, Washington, DC. EPA/600/R-090/052F.

USEPA. (2011b). Toxicological review of dichloromethane (methylene chloride). National Center for Environmental Assessment, Washington, DC, EPA/635/R-10/003F. www.epa.gov/iris

USEPA. (2014). Guidance for applying quantitative data to develop data-derived extrapolation factors for interspecies and intraspecies extrapolation. Office of the Science Advisor, Risk Assessment Forum. EPA/100/R-14/002F.

Villanueva, C.M., Kogevinas, M., Cordier, S,, Templeton, M.R., Vermeulen, R., Nuckols, J.R., Nieuwenhuijsen, M.J., and Levallois, P. (2014). Assessing exposure and health consequences of chemicals in drinking water: current state of knowledge and research needs. Environ. Health Perspect. 122, 213-221.

Xu, X., Mariano, T.M., Laskin, J.D., and Weisel, C.P. (2002). Percutaneous absorption of trihalomethanes, haloacetic acids, and haloketones. Toxicol. Appl. Pharmacol **184**, 19-26.

Yang, F., Tong, X., McCarver, D.G., Hines, R.N., and Beard, D.A. (2006). Population-based analysis of methadone distribution and metabolism using an age-dependent physiologically based pharmacokinetic model. J. Pharmacokinet. Pharmacodynam. 33, 485-518.

Young, J.F., Luecke, J.H., Pearce, B.A., Lee, T., Ahn, H., Baek, S., Moon, H., Dye, D.W., Davis, T.M., and Taylor, S.J. (2009). Human organ/tissue growth algorithms that include obese individuals and black/white population organ weight similarities from autopsy data. J. Toxicol. Environ. Health, Pt A. **72**, 527-540.

White, D.R., Widdowson, E.M., Woodard, H.Q., and Dickerson J.W.T. (1991). The composition of body tissues (II) fetus to young adult. Br. J. Radiology **64**, 149-159.

Yoon M., and Clewell, H.J. (2016). Addressing early life sensitivity using physiologically based pharmacokinetic modeling and in vitro to in vivo extrapolation. Toxicol. Res. **32**, 15-20.

Zhao G., and Allis J.W. (2002). Kinetics of bromodichloromethane metabolism by cytochrome P450 isoenzymes in human liver microsomes. Chem.-Biol. Interact. **140**, 155-168.

Table 1. Pediatric and Adult Physiological parameters for the human BDCM model

Parameter, units	Symbol	Child 0-30 days	Child 31-90 days	Child ~1-2 years	Adult	Note
Height, cm	height	51.8	57.4	81.0	174.7	[1]
Body Weight, kg	BW	3.81	5.22	10.55	80.8	[2]
Alveolar ventilation Rate, L/h-m^2	QPC	391	432	470	419	[3]
Alveolar Deadspace, unitless	deadspace	0.336	0.336	0.336	0.344	[3]
QPC to Cardiac Output (CO) Ratio, unitless	RQPCO	1.0	1.0	1.0	1.0	[4]
Fractional Blood Flows, unitless						
Richly Perfused Tissue Group	FQRP	0.75	0.75	0.75	0.75	[5, 7]
Liver	FQL	0.13	0.13	0.13	0.09	[5 ,6]
Gastrointestinal Tract	FQG	0.15	0.15	0.12	0.16	[5, 6]
Kidney	FQK	0.13	0.13	0.14	0.15	[5, 6]
Poorly Perfused Tissue Group	FQPP	0.25	0.25	0.25	0.25	[5, 7]
Fat	FQF	0.04	0.04	0.05	0.05	[5 ,6]
Blood Flow to Skin, L/min-m^2	QSKSA	0.58	0.58	0.58	0.58	[5, 7]
Compartment Volume, unitless						
Blood fraction of BW	FVBD	0.0671	0.0617	0.0529	0.079	[5,8]
Blood as arterial	FVART	0.25	0.25	0.25	0.25	[5]
Blood as venous	FVVEN	0.75	0.75	0.75	0.75	[5]
Richly perfused fraction of BW	FVRP	0.2	0.2	0.2	0.2	[5]
Poorly perfused fraction of BW	FVPP	0.8	0.8	0.8	0.8	[5]
GI tract fraction of BW	FVGI	0.0146	0.0146	0.0177	0.0165	[5, 8]
Liver fraction of BW	FVL	0.0355	0.0355	0.0382	0.026	[5, 8]
Fat fraction of BW	FVF	0.169	0.174	0.175	0.21	[8]
Kidney fraction of BW	FVK	0.0065	0.0065	0.0066	0.004	[5, 8]
Volume GI tract lumen, L	VLUM	0.14	0.14	0.24	2.1	[5, 9]
Skin thickness, mm	LSK	1.3	1.3	1.3	2.0	[5, 10]

[1]Calculated based on midpoint of age range for 50th percentile from CDC data tables for length-for-age for male and female children. https://www.cdc.gov/growthcharts/who_charts.htm#The WHO Growth Charts. For adult, used mean combined male and female, aged 30-40 years (Table 8-3, USEPA, 2011a).

[2]Calculated based on midpoint of age range for 50th percentile from CDC data tables for weight-for-age for male and female children. https://www.cdc.gov/growthcharts/who_charts.htm#The WHO Growth Charts. For adult used combined male and female, aged 30-40 mean (Table 8-16, USEPA, 2011a).

[3]Derived from mean of alveolar ventilation rate male and female children at ~ 1 month in Brochu *et al.* (2006), and 0.22-0.5 yrs for 30-90 dys group, 1-2 yrs of age and adults (35-40 yrs) in Brochu *et al.* (2011). Deadspace figures from Brochu *et al.*, (2012) with childhood age groups assumed same and set to mean value for youngest age group (5-10 years) and 35-45 year age group for adults. Minute ventilation rate is scaled to skin surface area (SA) in m^2 in the model; QP = QPC* SA * (1-Deadspace). SA = Height $^{(0.725)}$ * Weight $^{(0.425)}$ * 0.007187 in m^2 from (Adams, 1993; also eq. 6-3 in USEPA, 2008) for all childhood age groups. For adults use equation, SA = Height $^{(0.417)}$ * Weight $^{(0.517)}$ * 0.02350 in m^2 (Gehan and George, 1970, also eq. 7A-3 USEPA, 2011a).

[4]Cardiac Output, QC = QP/RQPCO.

[5]Adult value same as in original model.

[6]Blood flows calculated from Edginton *et al.* (2006) for 0-30 (newborn) and one year-old, 31-90 days assumed same as newborn. Fractional blood flows to individual tissues are scaled to cardiac output (QC), i.e. QL = FQL *QC, QG= FQG *QC, QK= FQK * QC, and QF = FQF * QC.

[7]Richly (QRP) and poorly perfused (QPP) tissues calculated by difference subtracting out blood flows from liver, kidney and gut for QRP and subtracting out fat and skin volumes for QPP, i.e., QRP = (FQRP*QC)-QL-QK-QG and QPP = (FQPP*QC)-QF-QSK.. Blood flow to skin (QSK) is scaled on the basis of body surface area, i.e., QSK = QSKSA * SA * 60 min/hr. Total liver blood flow is sum of liver plus gut as shown in Figure S1.

[8]Calculated as fraction of BW using estimated mass based on equations from Haddad *et al.*, (2001) using average of male and female and midpoint of age range. FVL is included for completeness; Monte Carlo analysis uses FVL distributional descriptors specific for each age group in Table 3. Blood volume assumes density of 1 g/L. Fat volume is recalculated from equations of Haddad *et al.*, (2001) based on modifications in Price *et al.* (2003). Volume of blood compartment is scaled to BW and volume of arterial and venous compartments are scaled to total blood volume. Tissue volumes to tissues are scaled to BW with richly (VRP) and poorly perfused (VPP) tissue volumes calculated respectively, as follows: VRP = FVRP*BW-VL-VGI-VBD-VK and VPP = FVPP*BW-VF-VSK. Volume of skin (VSK) is calculated as VSK = LSK*SA.

[9]Estimated based on figures in ICRP (2002, Table 2,8, p. 18) for newborn and 1-year old; age range 31-90 days assumed to be same as 0-30 days.

[10] LSK is average value for thickness of dermis and epidermis for adults (Laurent *et al.*, 2007) and all pediatric age groups (Ploin *et al.*, 2011). Note that skin thickness remains relatively unchanged based on age (up to 5 years), BMI, gender and skin phototype (Ploin *et al.*, 2011).

Table 2. Chemical-specific parameters in the human BDCM model*

Parameter, units	Symbol	Value	Footnote
Partition coefficients, unitless			
Blood:Air	PBBDCM	15.97	[1]
Liver:Blood	PLBDCM	1.93	[1]
Gut:Blood	PGBDCM	1.93	[2]
Kidney:Blood	PKBDCM	2.08	[1]
Fat:Blood	PFBDCM	33.2	[1]
Skin:Blood	PSKBDCM	2.91	[3]
RPTG:Blood	PRPBDCM	1.93	[2]
PPTG:Blood	PPPBDCM	0.78	[1]
Skin diffusion coefficient, cm/h	KBDCM	0.18	[4]
Skin:water partition coefficient	PWSBDCM	5.6	[4]
Oral absorption coefficient, h^{-1}	KABDCM	8.3	[5]
Vmax CYP Liver, µg/h-pmol CYP2E1	IVVMAX	0.201	[6]
KM CYP Liver, µg/L	KM1BDCM	221	[6]
Kf GST Liver, 1/h-kg $BW^{0.75}$	VFCBDCM	0.0079	[7]

[1]Calculated by dividing rat tissue:air partition coefficient (Lilly *et al.* 1997) by human blood:air partition coefficient from Kenyon *et al*. (2016).

[2] Gut:air and rapidly perfused tissue:air partition coefficients were assumed to be the same as liver:air.

[3] Skin:air partition coefficient (Haddad *et al.* 2006) used with human blood air partition coefficient to calculate skin:blood partition coefficient.

[4] Skin diffusion coefficient determined with method using aqueous solution across human skin (Xu *et al.* 2002). Skin:water partition coefficient calculated on basis of water:air partition coefficient (Batterman *et al.* 2002) divided by skin:air partition coefficient (Haddad *et al.* 2006).

[5]Estimated on basis of Tmax from oral time course data of Leavens *et al.* (2007) and assumed to be the same across age groups.

[6]Experimentally determined in pooled adult human microsomes as 1.74 nmoles/min – mg MSP (Kenyon *et al.*, 2016a) and converted to 17.14 µg/h-mg MSP in (Kenyon *et al.*, 2016b) analysis. Converted to basis of CYP 2E1 for this analysis using known average CYP2E1 content (85 pmol CYP2E1/mg MSP) for independent set of adult samples for which both CYP2E1 content and P450 content are known at the level of the individual subject (J. Lipscomb, personal communication).

[7]Estimated from *in vitro* clearance of BDCM from pooled human liver cytosol (Ross and Pegram 2003).

Table 3. Parameter distributions and values used as input to Monte Carlo analysis for pediatric age groups and adults

Parameters[1]	FVL		MPPGL		CYP2E1	
Age Group	Distribution & Descriptors[2]	Value	Distribution & Descriptors	Value	Distribution & Descriptors	Value
0-30 days, neonate	Normal		Log Normal		Gamma	
	Mean	0.0412	GM	25.55	Alpha	0.505
	SD	0.0157	GSD	1.001	Theta	26.6
	Lower Limit	0.0114	Lower Limit	25.53		
	Upper Limit	0.0775	Upper Limit	25.60		
31-90 days, infant	Normal		Log Normal		Gamma	
	Mean	0.0366	GM	25.68	Alpha	10.7
	SD	0.0102	GSD	1.002	Theta	2.24
	Lower Limit	0.0145	Lower Limit	25.61		
	Upper Limit	0.0612	Upper Limit	25.74		
91 days – 2 years, toddler	Normal		Log Normal		Gamma	
	Mean	0.0445	GM	26.35	Alpha	4.82
	SD	0.0159	GSD	1.028	Theta	9.42
	Lower Limit	0.0274	Lower Limit	25.76		
	Upper Limit	0.1200	Upper Limit	27.36		
Adult	Normal		Log Normal		Gamma	
	Mean	0.0239	GM	35.24	Alpha	11.1
	SD	0.0090	GSD	1.094	Theta	5.33
	Lower Limit	0.0136	Lower Limit	29.26		
	Upper Limit	0.0415	Upper Limit	40.19		

[1]FVL (g liver/kg BW, assuming a volumetric density of 1) and CYP2E1 (pmol/mg microsomal protein) were calculated from data in Johnsrud *et al.* (2003) for specific pediatric age groups. FVL for adults was recalculated from Young *et al.* (2009). CYP2E1 for adults is from Lipscomb *et al*. (1997, 2003a, b). MPPGL was estimated on the basis of the equation published in Barter *et al.* (2008) using subject age in years for all age groups.

[2]Lower and upper limits are lowest and highest values from data, respectively. Abbreviations: SD is standard deviation, GM is geometric mean and GSD is geometric standard deviation. GM and GSD are log transformed for input into acslx MC routines. For the gamma distribution, alpha is the shape parameter and theta is the scale parameter.

Table 4. Statistical characteristics for maximum concentration of BDCM in blood (CvMax) based on Monte Carlo analysis following oral exposure (single 0.05 L drink, 5 µg/L BDCM in water, 2 hr simulation).

Age Group	Mean ± SD (ng/L)	% CV	5th percentile	95th percentile	Ratio[1]
neonate	24.1 ± 19.1	79.2	2.57	58.6	22.8
infant	5.39 ± 2.09	38.7	2.83	9.28	3.28
toddler	1.32 ± 0.77	57.9	0.52	2.75	5.28
adult	0.23 ± 0.10	43.4	0.11	0.41	3.75

[1]Ratio of 95th to 5th percentile values.

Table 5. Statistical characteristics for maximum concentration of BDCM in blood (CvMax) based on Monte Carlo analysis following bathing exposure (20 minutes, 5 µg/L BDCM in water, 2 hr simulation).

Age Group	Mean ± SD (ng/L)	% CV	5th percentile	95th percentile	Ratio[1]
neonate	86.8 ± 23.0	26.5	63.53	132.3	2.08
infant	61.8 ± 2.35	3.80	59.06	66.20	1.12
toddler	56.5 ± 1.39	2.45	55.17	59.08	1.07
adult	49.0 ± 0.49	1.00	48.39	49.87	1.03

[1]Ratio of 95th to 5th percentile values.

Table 6. Intragroup and adult-child variability factors derived from AUC for BDCM in venous blood (AUCv) for pediatric age groups and adults for bathing and oral scenarios (5 µg/L BDCM in water)

Age Group	Scenario	AUCv (µg-h/L)			Intragroup Factor[1]	Adult-child Factor[2]
		5th%	50th%	95th		
Neonate	Bath	0.0270	0.0351	0.0940	2.68	3.55
Infant		0.0252	0.0265	0.0294	1.11	1.11
Toddler		0.0238	0.0244	0.0261	1.07	0.99
Adult		0.0260	0.0265	0.0276	1.04	
Neonate	Oral	7.26E-04	5.70E-03	4.31E-02	7.57	558
Infant		8.02E-04	1.46E-03	2.92E-03	2.00	37.8
Toddler		1.52E-04	3.42E-04	8.60E-04	2.52	11.1
Adult		3.95E-05	7.72E-05	1.59E-04	2.06	

[1]The intragroup variability factor was calculated as the ratio of the 95th percentile value over the 50th percentile value for the same age group.

[2]The adult-child variability factor was calculated as the ratio of the 95th percentile value for the child over the 50th percentile value for the adult.

Table 7. Intragroup and adult-child variability factors derived from amount of BDCM metabolized in liver (AML) for pediatric age groups and adults for bathing and oral scenarios (5 µg/L BDCM in water)

Age Group	Scenario	AML (µg)			Intragroup Factor[1]	Adult-child Factor[2]
		5th%	50th%	95th		
Neonate	Bath	0.023	0.358	0.401	1.12	0.12
Infant		0.464	0.486	0.495	1.02	0.15
Toddler		0.799	0.825	0.834	1.01	0.25
Adult		3.275	3.345	3.377	1.01	
Neonate	Oral	0.014	0.220	0.246	1.12	1.00
Infant		0.229	0.240	0.244	1.02	0.99
Toddler		0.238	0.245	0.248	1.01	1.01
Adult		0.241	0.246	0.248	1.01	

[1]The intragroup variability factor was calculated as the ratio of the 95th percentile value over the 50th percentile value for the same age group.

[2]The adult-child variability factor was calculated as the ratio of the 95th percentile value for the child over the 50th percentile value for the adult.

Figure Legends

Fig 1. Diagram illustrating workflow and methodology. The model and subsequent analyses were implemented in acslXtreme 3.0.2.1 (The AEgis Technologies Group; Huntsville, AL).

Fig 2. Comparison of AUC for (A) venous blood BDCM (µg-h/L, $\bar{x} \pm$ SD) and (B) amount of BDCM metabolized in liver (µg, $\bar{x} \pm$ SD) across age groups based on Monte Carlo simulations (2 hours) utilizing the distributional characteristics for FVL, CYP2E1 and MPPGL shown in Table 3 for an oral exposure to water containing 5 µg/L BDCM as a single 0.05-liter drink. The number associated with each bar is the coefficient of variation (%).

Fig 3. Comparison of AUC for (A) venous blood BDCM (µg-h/L, $\bar{x} \pm$ SD) and (B) amount BDCM metabolized in liver (µg, $\bar{x} \pm$ SD) across age groups based on Monte Carlo simulations (2 hours) utilizing the distributional characteristics for FVL, CYP2E1 and MPPGL shown in Table 3 for a 20-minute bath in water containing 5 µg/L BDCM. The number associated with each bar is the coefficient of variation (%).

Fig 4. Morris screening level global sensitivity analysis for oral exposure scenario of a single 0.05 L ingestion of water containing 5 µg/L BDCM for AUCv in (A) neonate and (B) adult. Parameter abbreviations are defined in Tables 1 and 2. Due to space constraints, only the most influential parameters were annotated.

Fig 5. Morris screening level global sensitivity analysis for oral exposure scenario of a single 0.05 L ingestion of water containing 5 µg/L BDCM for AML in (A) neonate and (B) adult. Parameter abbreviations are defined in Tables 1 and 2. Due to space constraints, only the most influential parameters were annotated.

Fig 6. Morris screening level global sensitivity analysis for bathing exposure for 20 minutes in water containing 5 µg/L BDCM for AUCv in (A) neonate and (B) adult. Parameter abbreviations are defined in Tables 1 and 2. Due to space constraints, only the most influential parameters were annotated.

Fig 7. Morris screening level global sensitivity analysis for bathing exposure for 20 minutes in water containing 5 µg/L BDCM for AML in (A) neonate and (B) adult. Parameter abbreviations are defined in Tables 1 and 2. Due to space constraints, only the most influential parameters were annotated.

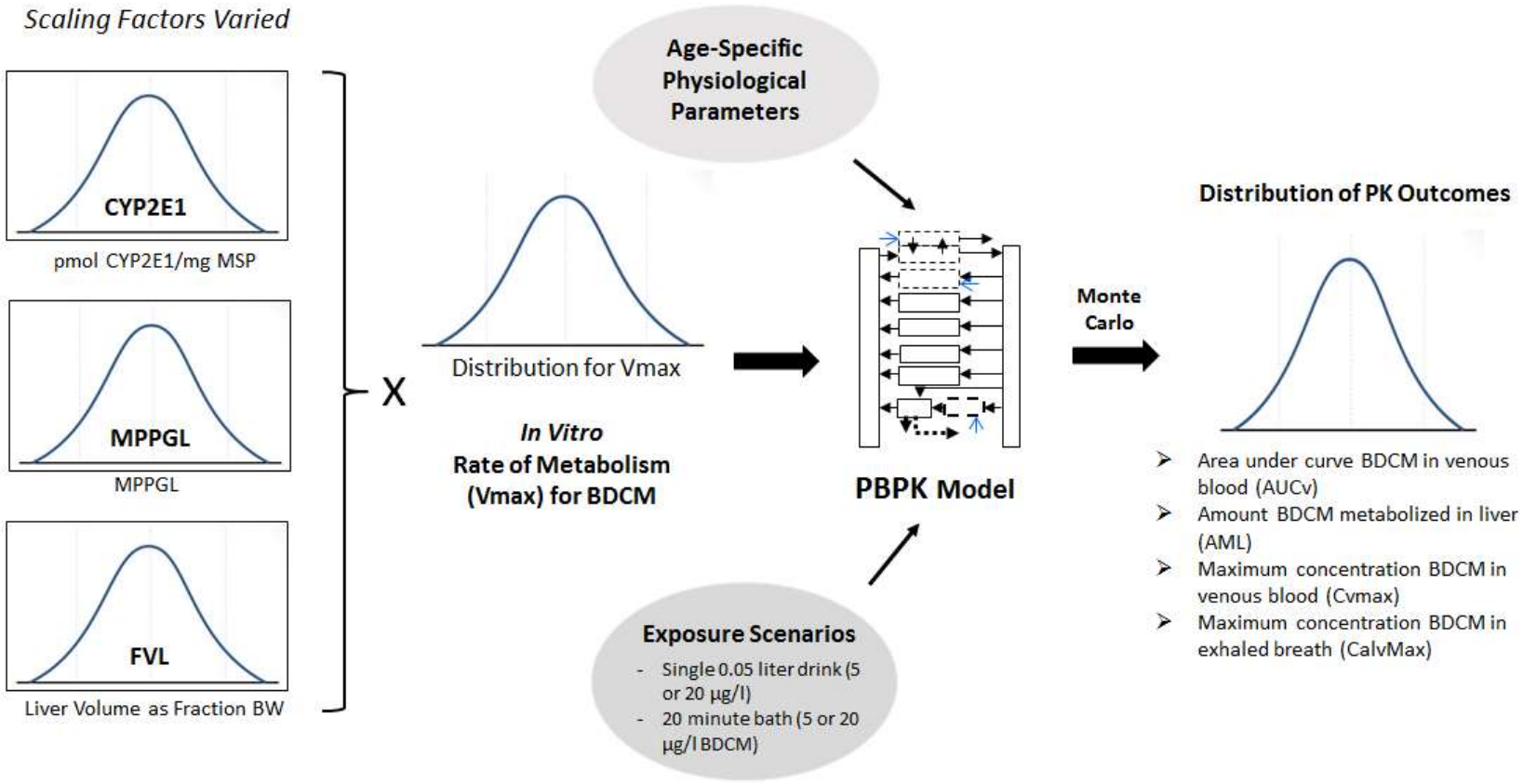
Scaling Factors Varied
CYP2E1
pmol CYP2E1/mg MSP
MPPGL
MPPGL
FVL
Liver Volume as Fraction BW
X
Distribution for Vmax
In Vitro
Rate of Metabolism
(Vmax) for BDCM
Age-Specific
Physiological
Parameters
PBPK Model
Exposure Scenarios
- Single 0.05 liter drink (5 or 20 µg/l)
- 20 minute bath (5 or 20 µg/l BDCM)
Monte
Carlo
Distribution of PK Outcomes
Area under curve BDCM in venous blood (AUCv)
Amount BDCM metabolized in liver (AML)
Maximum concentration BDCM in venous blood (Cvmax)
Maximum concentration BDCM in exhaled breath (CalvMax)

Figure 1

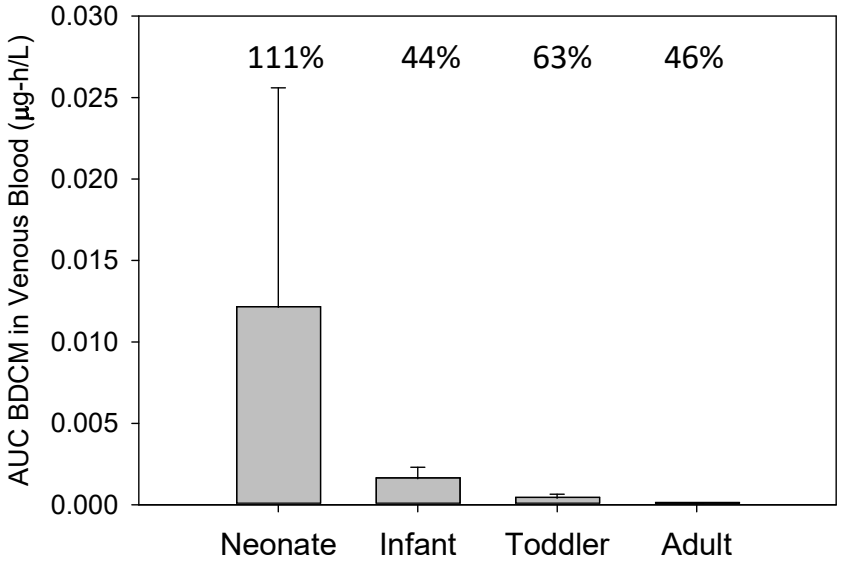

Figure 2A

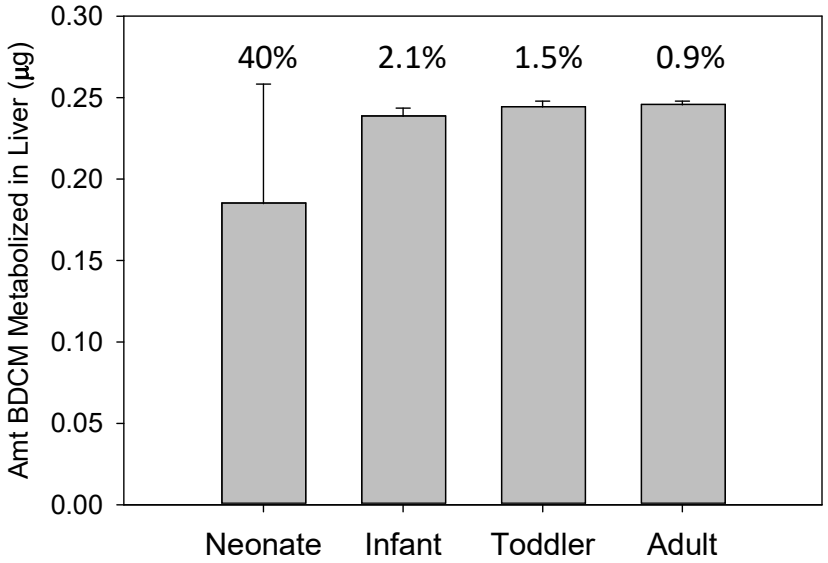

Figure 2B

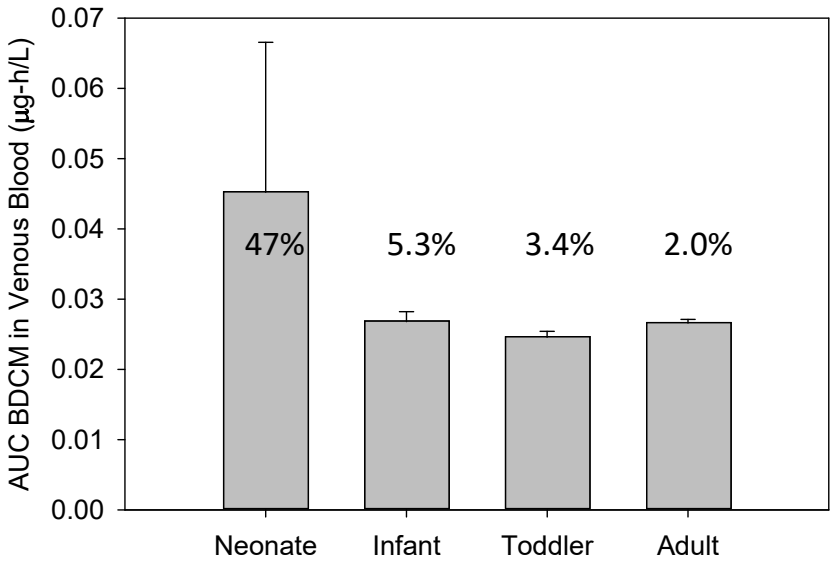

Figure 3A

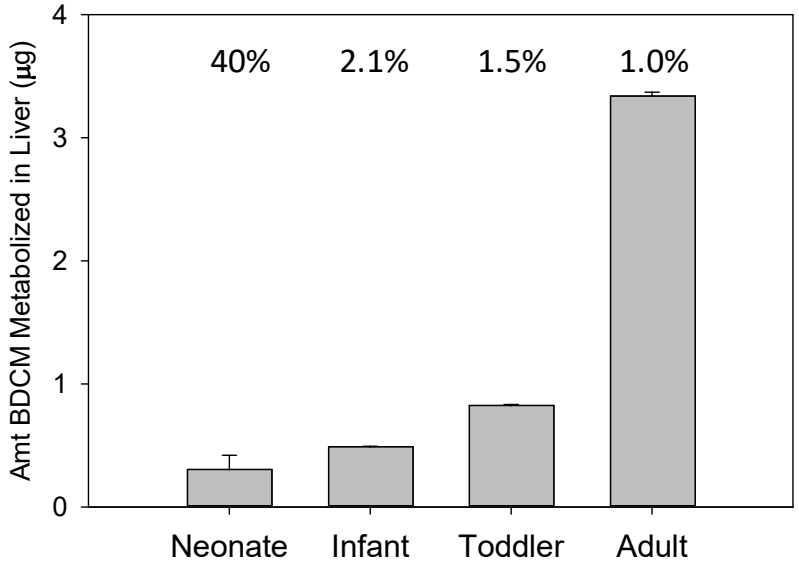

Figure 3B

A

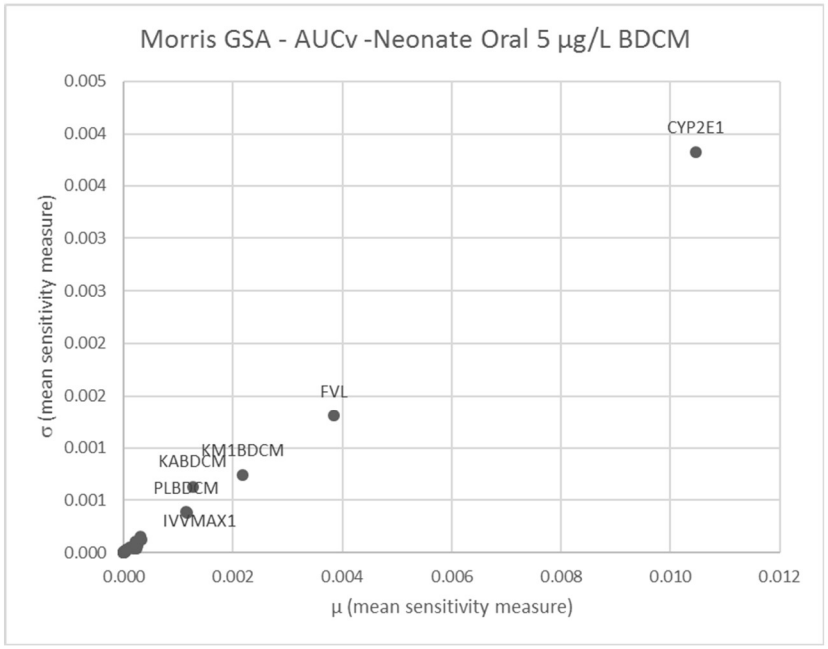
Morris GSA - AUCv -Neonate Oral 5 µg/L BDCM
σ (mean sensitivity measure)
µ (mean sensitivity measure)
CYP2E1
FVL
KM1BDCM
KABDCM
PLBDCM
IVVMAX1
0.005
0.004
0.004
0.003
0.003
0.002
0.002
0.001
0.001
0.000
0.000
0.002
0.004
0.006
0.008
0.010
0.012

B

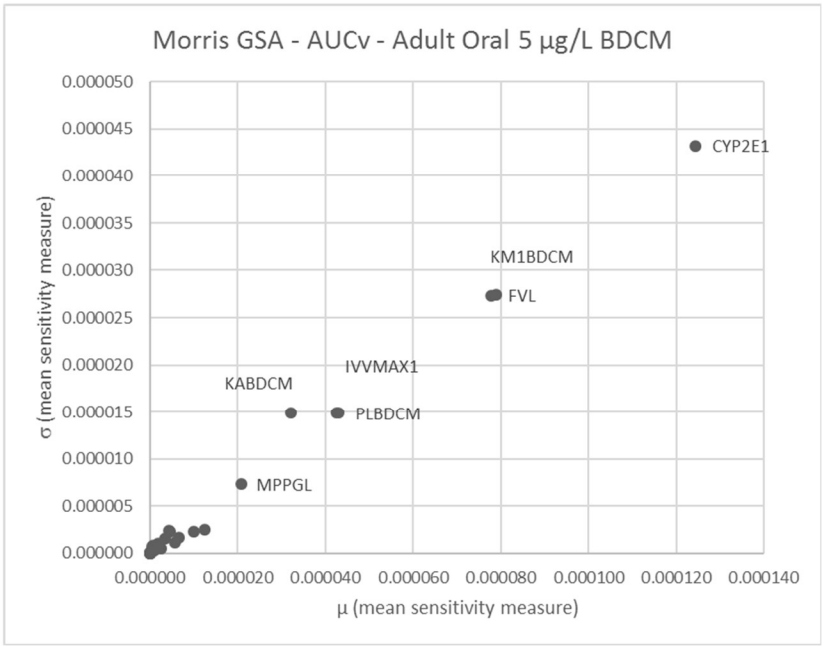
Morris GSA - AUCv - Adult Oral 5 µg/L BDCM
σ (mean sensitivity measure)
µ (mean sensitivity measure)
CYP2E1
KM1BDCM
FVL
IVVMAX1
KABDCM
PLBDCM
MPPGL
0.000050
0.000045
0.000040
0.000035
0.000030
0.000025
0.000020
0.000015
0.000010
0.000005
0.000000
0.000000
0.000020
0.000040
0.000060
0.000080
0.000100
0.000120
0.000140

Figure 4

A

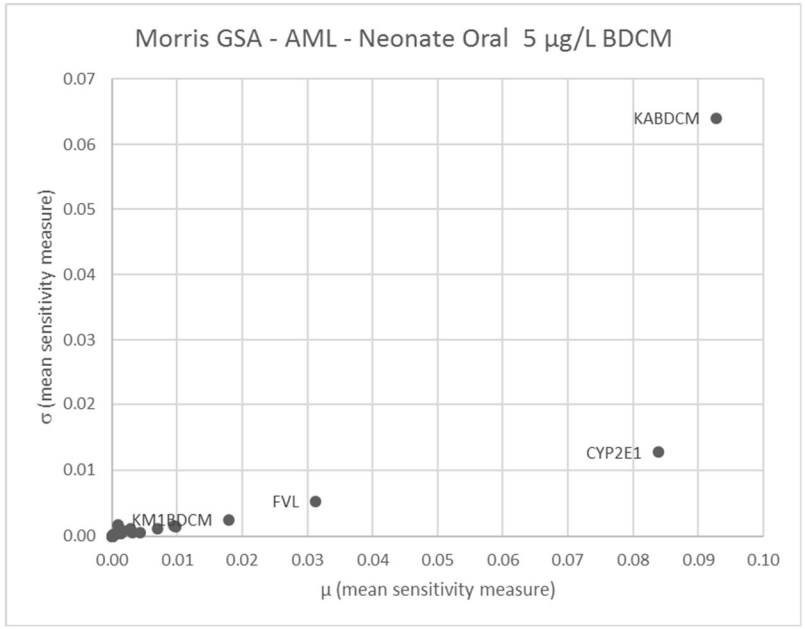
Morris GSA - AML - Neonate Oral 5 µg/L BDCM
σ (mean sensitivity measure)
µ (mean sensitivity measure)
KABDCM
CYP2E1
FVL
KM1BDCM
0.00
0.01
0.02
0.03
0.04
0.05
0.06
0.07
0.08
0.09
0.10

B

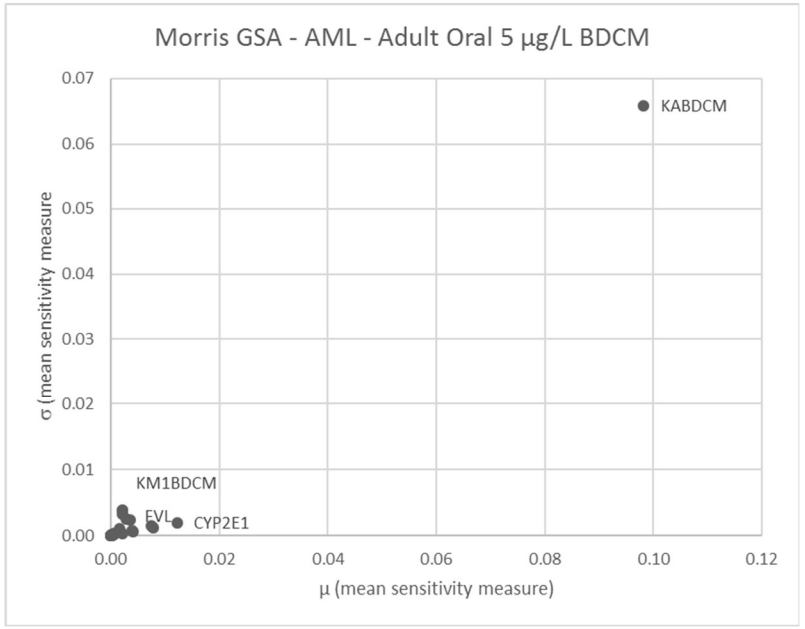
Morris GSA - AML - Adult Oral 5 µg/L BDCM
σ (mean sensitivity measure
µ (mean sensitivity measure)
KABDCM
KM1BDCM
FVL
CYP2E1
0.00
0.02
0.04
0.06
0.08
0.10
0.12

Figure 5

A

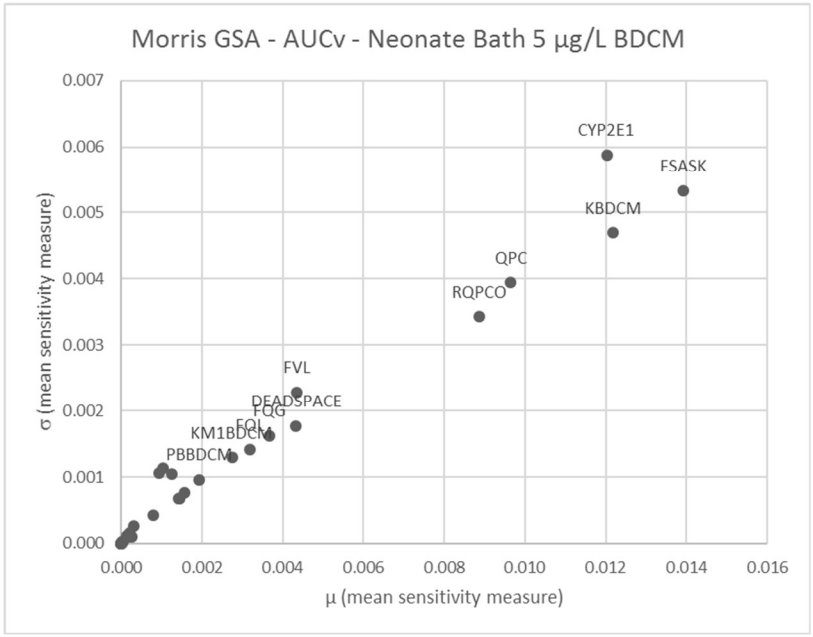
Morris GSA - AUCv - Neonate Bath 5 µg/L BDCM
σ (mean sensitivity measure)
µ (mean sensitivity measure)
0.007
0.006
0.005
0.004
0.003
0.002
0.001
0.000
0.000
0.002
0.004
0.006
0.008
0.010
0.012
0.014
0.016
CYP2E1
FSASK
KBDCM
QPC
RQPCO
FVL
DEADSPACE
FQG
FQL
KM1BDCM
PBBDCM

B

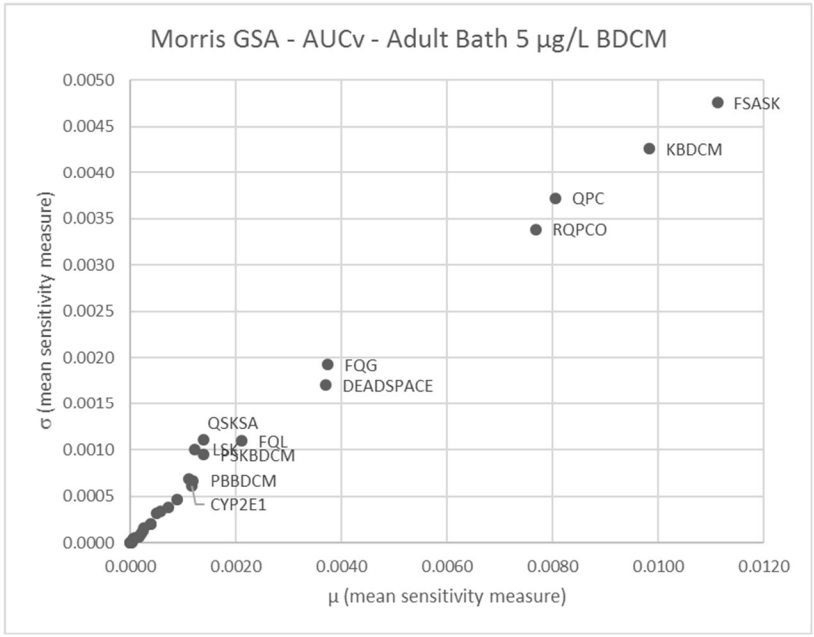
Morris GSA - AUCv - Adult Bath 5 µg/L BDCM
σ (mean sensitivity measure)
µ (mean sensitivity measure)
0.0050
0.0045
0.0040
0.0035
0.0030
0.0025
0.0020
0.0015
0.0010
0.0005
0.0000
0.0000
0.0020
0.0040
0.0060
0.0080
0.0100
0.0120
FSASK
KBDCM
QPC
RQPCO
FQG
DEADSPACE
QSKSA
FQL
PBBDCM
CYP2E1

Figure 6

A

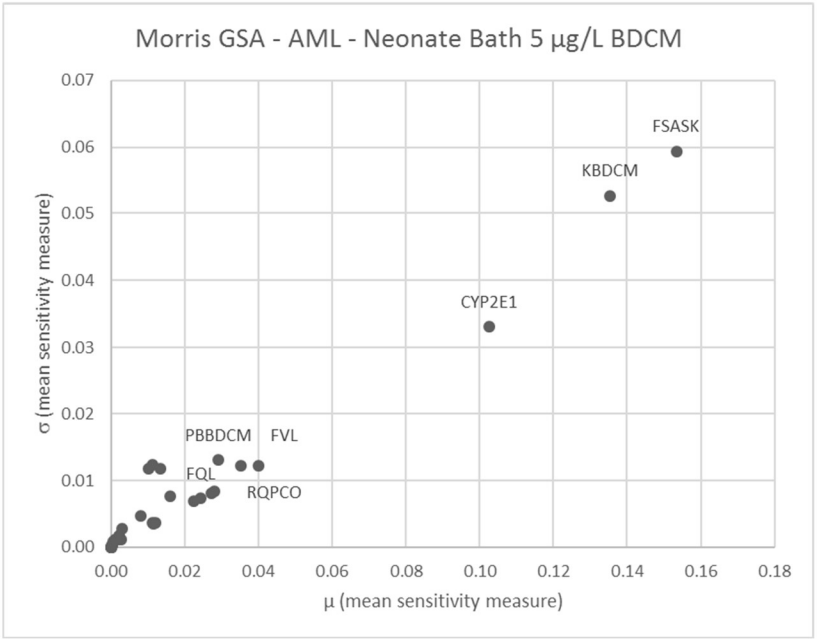
Morris GSA - AML - Neonate Bath 5 µg/L BDCM
σ (mean sensitivity measure)
µ (mean sensitivity measure)
0.00
0.01
0.02
0.03
0.04
0.05
0.06
0.07
0.00
0.02
0.04
0.06
0.08
0.10
0.12
0.14
0.16
0.18
FSASK
KBDCM
CYP2E1
PBBDCM
FVL
FQL
RQPCO

B

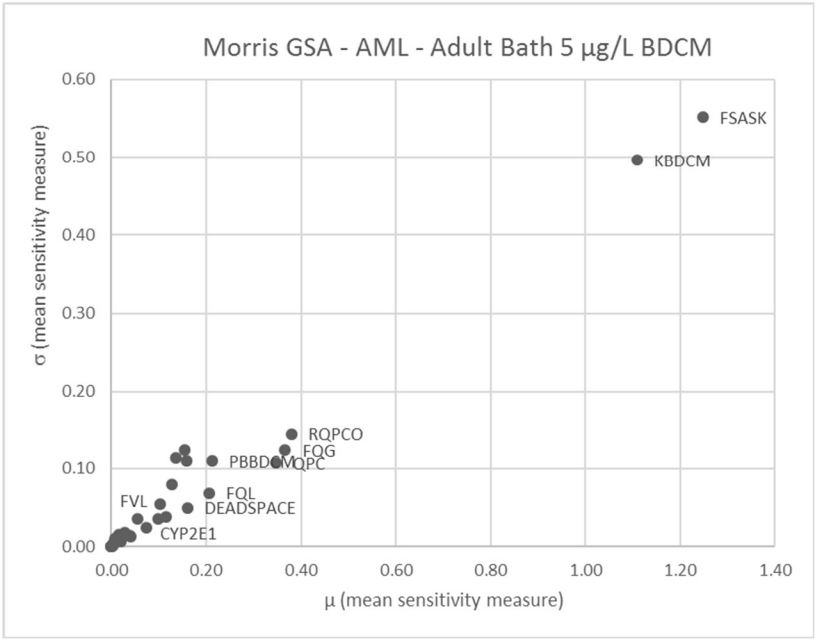
Morris GSA - AML - Adult Bath 5 µg/L BDCM
σ (mean sensitivity measure)
µ (mean sensitivity measure)
0.00
0.10
0.20
0.30
0.40
0.50
0.60
0.00
0.20
0.40
0.60
0.80
1.00
1.20
1.40
FSASK
KBDCM
RQPCO
FQG
PBBDCM
MQPC
FQL
DEADSPACE
FVL
CYP2E1

Figure 7